



COMPLIMENTARY/POSTER SESSION PAPER

Interspecific Differences in the Flow Regimes and Drag of North Pacific Skate Egg Cases

Kayla C. Hall^{*†,1}, Jaida N. Elcock^{‡§}, Gerald R. Hoff[¶], Duane E. Stevenson^{||}, Adam P. Summers^{*†}
and Cassandra M. Donatelli^{*||}

*Friday Harbor Labs, University of Washington, 620 University Road, Friday Harbor, WA 98250, USA; †Department of Biology, University of Washington, Life Sciences Building, W Stevens Way NE Seattle, WA 98195, USA; ‡Department of Biology, Woods Hole Oceanographic Institution, Woods Hole Road, MS 31, Clark 223, Woods Hole, MA 02543, USA; §Department of Earth and Planetary Science, Massachusetts Institute of Technology, 77 Massachusetts Ave 54-918, Cambridge, MA 02139, USA; ¶NOAA, National Marine Fisheries Service, Alaska Fisheries Science Center, 7600 Sand Point Way NE, Seattle, WA 98115, USA; ||Fowler School of Engineering, Chapman University, 1 University Dr, Orange, CA 92866, USA

From the symposium “Integrating ecology and biomechanics to investigate patterns of phenotypic diversity: Evolution, development, and functional traits” presented at the annual meeting of the Society for Integrative and Comparative Biology virtual annual meeting, January 3–February 28, 2022.

¹Email: kchall8@uw.edu

Synopsis Skates are a diverse group of dorso-ventrally compressed cartilaginous fish found primarily in high-latitude seas. These slow-growing oviparous fish deposit their fertilized eggs into cases, which then rest on the seafloor. Developing skates remain in their cases for 1–4 years after they are deposited, meaning the abiotic characteristics of the deposition sites, such as current and substrate type, must interact with the capsule in a way to promote long residency. Egg cases are morphologically variable and can be identified to species. Both the gross morphology and the microstructures of the egg case interact with substrate to determine how well a case stays in place on a current-swept seafloor. Our study investigated the egg case hydrodynamics of eight North Pacific skate species to understand how their morphology affects their ability to stay in place. We used a flume to measure maximum current velocity, or “break-away velocity,” each egg case could withstand before being swept off the substrate and a tilt table to measure the coefficient of static friction between each case and the substrate. We also used the programming software R to calculate theoretical drag on the egg cases of each species. For all flume trials, we found the morphology of egg cases and their orientation to flow to be significantly correlated with break-away velocity. In certain species, the morphology of the egg case was correlated with flow rate required to dislodge a case from the substrate in addition to the drag experienced in both the theoretical and flume experiments. These results effectively measure how well the egg cases of different species remain stationary in a similar habitat. Parsing out attachment biases and discrepancies in flow regimes of egg cases allows us to identify where we are likely to find other elusive species nursery sites. These results will aid predictive models for locating new nursery habitats and protective policies for avoiding the destruction of these nursery sites.

Introduction

Skates (Rajiformes) are the most speciose superorder of all cartilaginous fish, comprised of roughly 280 species (Ebert and Winton 2010; Chiquillo et al. 2014), yet a great deal of their ecological preferences remain unknown. All skates are slow-growing oviparous fish that deposit their eggs in capsules onto the seafloor where

they remain throughout embryonic development for a period of 1–4 years, depending on species (Wourms 1977; Hoff 2008, 2009; Ebert and Winton 2010). Some species in the North Pacific use nursery sites—locations where adults gather to deposit eggs at densities anywhere from 500 to 800,500 eggs/km² (Hoff 2008, 2010). There are currently 26 known nursery sites for six

Advance Access publication July 4, 2022

© The Author(s) 2022. Published by Oxford University Press on behalf of the Society for Integrative and Comparative Biology. All rights reserved. For permissions, please e-mail: journals.permissions@oup.com

species of skates in the eastern Bering Sea (Rooper et al. 2019). Maximum entropy models have shown that there is a limited area of the upper continental slope where conditions would likely support nursery areas (Rooper et al. 2019), but most of these regions remain unexplored and unprotected. There are 16 species of skates known to inhabit various geographical zones throughout the eastern North Pacific, ranging from the Salish Sea in northern Washington to the Gulf of Alaska, Aleutian Islands, and Bering Sea (Stevenson et al. 2007). Though egg cases are morphologically variable and can be identified to species (Stevenson et al. 2007; Ishihara et al. 2012), they all have a similar general anatomy with a large main body and hollow “horn” structures which allow seawater to flow through the body of the case (Fig. 2; Koob and Summers 1996; Long and Koob 1997). Both the gross morphology and the microstructure of the egg case interact with substrate to determine how well a case stays in place on a current-swept seafloor (Vogel 1994). Our goal is to use computational and physical hydrodynamic tests of flow and friction, coupled with geographic information system (GIS) data, to predict the locations of undocumented nursery sites in the North Pacific. Break-away velocity, or the flow velocity which causes an egg case to lift off of the seafloor, can be incorporated into fine-scale maps of potential habitats to rule out areas as prospective nursery sites. This will inform management strategies that protect these areas and the species that use them. The ecological preferences of these skates, in part determined by specific life-history stages, make them highly susceptible to trawling and long-line fishing, as these generally take place at continental shelf depths.

Our current understanding of the hydrodynamics of egg cases is limited to one quantitative account by Koob and Summers (1996). The authors measured the relative drag vs orientation for little skate (*Leucoraja erinacea*) egg cases. Their results showed that the lowest relative drag occurred when the long axis of the case was parallel to flow (anterior–posterior orientation) due to the streamlined shape. The egg cases experienced higher relative drag when oriented perpendicular to flow in a lateral orientation. In addition to flow around the case, they found that water flows through the capsule via the horn slits, which open about $\frac{1}{3}$ into development. These hydrodynamic properties are thought to enhance survival by providing consistent oxygen to satisfy the increasing respiratory demands as development progresses (Koob and Summers 1996).

Egg cases have been found in habitats where flow is as slow as 1 cm/s (Sigler et al. 2015; Reichert 2020). Embryos are able to oxygenate their egg cases in such a low current environment by actively creating flow through the horn slits with an embryonic-stage specific transi-

tory tail appendage (Long and Koob 1997). Long and Koob (1997) found that little skates beat their tails, producing waves of regular amplitude and axial curvature. The tail pumping generates a positive pressure in the horn occupied by the tail, which then causes a negative pressure in the unoccupied horns (Long and Koob 1997). This system causes water to exit the occupied horn and fill the three empty horns (Long and Koob 1997). The tail pump system appears to be co-adapted for ventilating the capsule, as the horns alone do not circulate enough new oxygenated water within the case. It is proposed that tail pump ventilation increases as passive flow within the capsule decreases, due to the embryos growing and taking up more volume (Long and Koob 1997).

To properly implement management strategies for a skate population we need to understand how they live and move through their environment. If we are to build upon predictive models, (i.e., Rooper et al. 2019), we need a better sense of what skates do across all life stages. For example, juvenile and adult Alaska skates (*Bathyraja parmifera*) occupy different portions of the habitat (Hoff 2008). Further, adults are known to frequent shallow depths of 30 m but are also found at depths from 145 to 380 m, which is where their nursery sites are located (Fig. 1; Hoff 2008, 2010, and Hoff pers comm). Nursery sites in canyon slope areas are heavily fished via trawls and longlines (Stevenson et al. 2019), increasing risk to crucial life stages: females laying eggs and developing embryos. Meanwhile, neonates and juvenile skates exhibit dramatic emigrations from nursery sites to avoid predators (Hoff 2010, 2016). Evaluating habitat and substrate effects are essential for pinpointing and protecting hotspots where skates are most likely to deposit eggs. For example, only a single nursery site has been found for *Beringrāja binocolata*, one of two species that houses multiple embryos per capsule (Hitz 1964). The *B. binocolata* nursery site was found at a relatively shallow depth of 65 m off the Oregon coast (Fig. 1, Fig. 6, Supplementary Table 1; Hitz 1964). Thus, any new or altered environmental stress, either natural or anthropogenic, could endanger this and additional unknown nursery sites for this migrating population. In 2014, the North Pacific Fishery Management Council designated six habitat areas of particular concern (HAPC) for skate nurseries in the eastern Bering Sea, recognizing their uniqueness and importance as essential nursery sites and fish habitats, yet many remain unprotected (Melton et al. 2014; Rooper et al. 2019). A recent analysis of bycatch data indicated that fishing gear is being deployed in and near skate nursery sites, including designated HAPC locations (Stevenson et al. 2019). Therefore, it is necessary to map skate habitats more distinctly to better inform fisheries management and

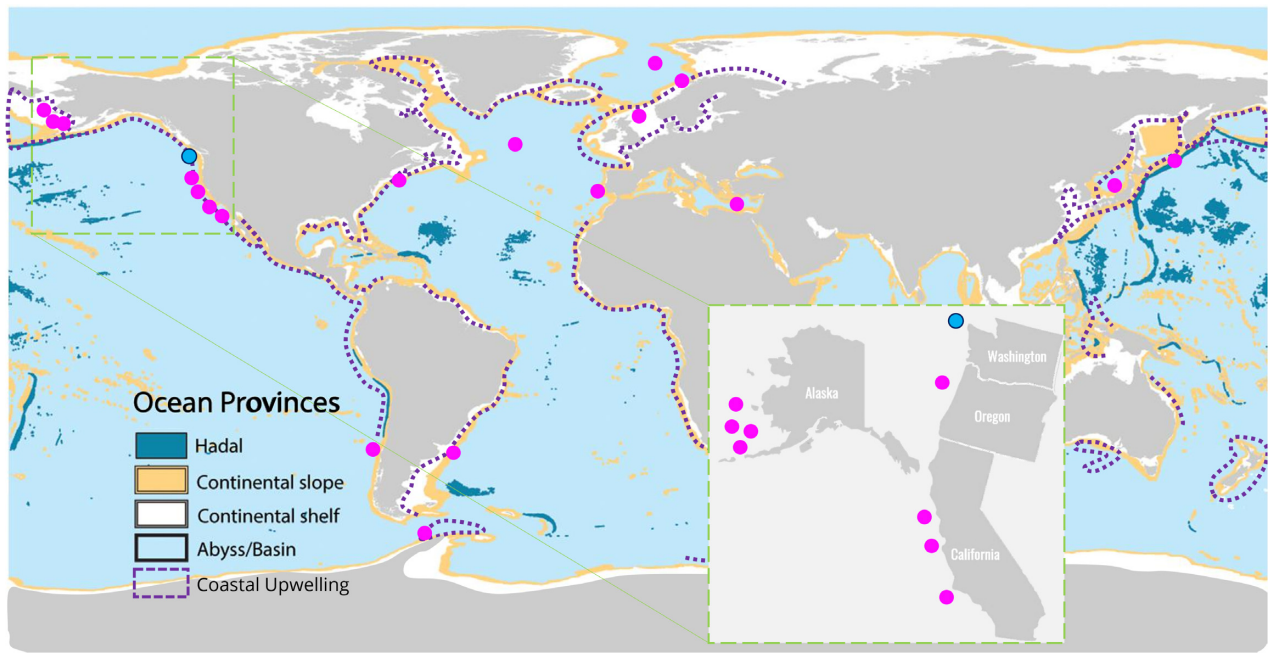


Fig. 1 Distribution of elasmobranch egg case nursery sites. Pink dots indicate the 20 sites found from literature sources (see Supplementary Table 1). The blue dot, off the coast of Washington, is the region we propose as a nursery site for *B. binoculata* and *R. rhina*. The inset indicates the nursery sites of the eight species used in this study.

implement strategies for bycatch reduction at specific life stages.

The aims of this study are three-fold: (a) to describe and compare the gross morphology of the egg cases as well as microstructures covering the surface; (b) to test the hydrodynamic and frictional forces skate egg cases are capable of withstanding, before breaking away from the substrate; (c) to use these data in conjunction with ecological and oceanographic surveys to inform predictions about potential nursery sites.

Methods

We compiled the global distribution and characteristics of elasmobranch egg case nursery sites from peer-reviewed literature sources (see Supplementary Table 1). We plotted these data on a map (Fig. 1; adapted from Atwood et al. 2020) with the addition of zones of coastal upwelling, following National Oceanic and Atmospheric Administration (NOAA) upwelling maps, and the locations of nursery sites (see Supplementary Table 1).

Morphology and morphometrics

We gathered physical data on preserved egg cases from eight North Pacific species: *Bathyraja aleutica*, *B. interrupta*, *B. minispinosa*, *B. parmifera*, *B. trachura*, and *B. taranetzi* are from the Aleutian Islands and eastern Bering Sea; *Beringraja binoculata* and *Raja rhina* are

found throughout the northeast Pacific Ocean. All egg cases were preserved in 70% ethanol. We selected undamaged egg cases, with yolk and/or embryo, for the trials.

Prior to testing, we gathered morphometrics of each individual egg case, including the total length (TL), case length (CL), width (W), and height (H), followed by macrophotography (Fig. 2). In each image the egg case was isolated from the background in Microsoft Photos (Microsoft Corporation, Redmond, WA, USA). We transformed the image to black/white via the threshold function in Fiji (Schindelin et al. 2012) and used the Magic Wand tool to collect the projected area of dorsal, anterior/posterior, and lateral views (Fig. 2).

Friction trials

Friction between two materials can be described by the static friction coefficient (μ ; Bowden and Tabor 1950). We measured the coefficient of static friction on the preserved specimens using a motorized metal tilt table, controlled by a programmable circuit board Arduino (Arduino, Torino, Italy). Egg cases were placed on the tilt table in the air on wet sandpaper (60 grit), which was attached with magnets to the tilt table, to simulate sediment (Fig. 3A). The table was tilted at a rate of $0.273^\circ/\text{s}$ until the egg case slid off, and the angle was recorded by a Johnson's magnetic angle locator. The coefficient of static friction (μ), can be calculated from the angle

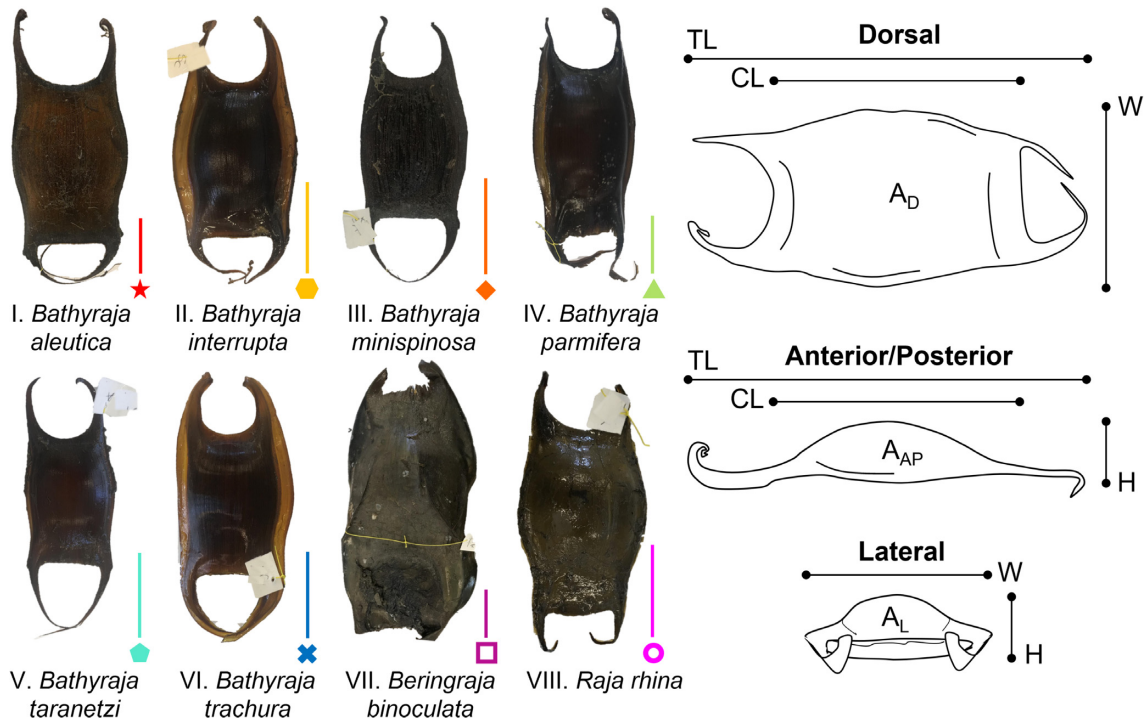


Fig. 2 Gross morphology and morphometrics of skate egg cases used in this study. The scale bar is 5 cm and color-coded specific to species, symbol is also species specific: Magenta star—I. *Bathyrāja aleutica*, Gold hexagon—II. *Bathyrāja interrupta*, Orange diamond—III. *Bathyrāja minispinosa*, Lime triangle—IV. *Bathyrāja parmifera*, Aqua pentagon—V. *Bathyrāja trachura*, Blue X—VI. *Bathyrāja taranetzi*, Purple square—VII. *Beringrāja binoculata*, and Pink circle—VIII. *Raja rhina*. The morphometrics of each individual egg case were gathered to include the total length (TL), case length (CL), width (W), and height (H). The dorsal area (AD), anterior–posterior area (AAP), and lateral area (AL) were collected for each individual as well.

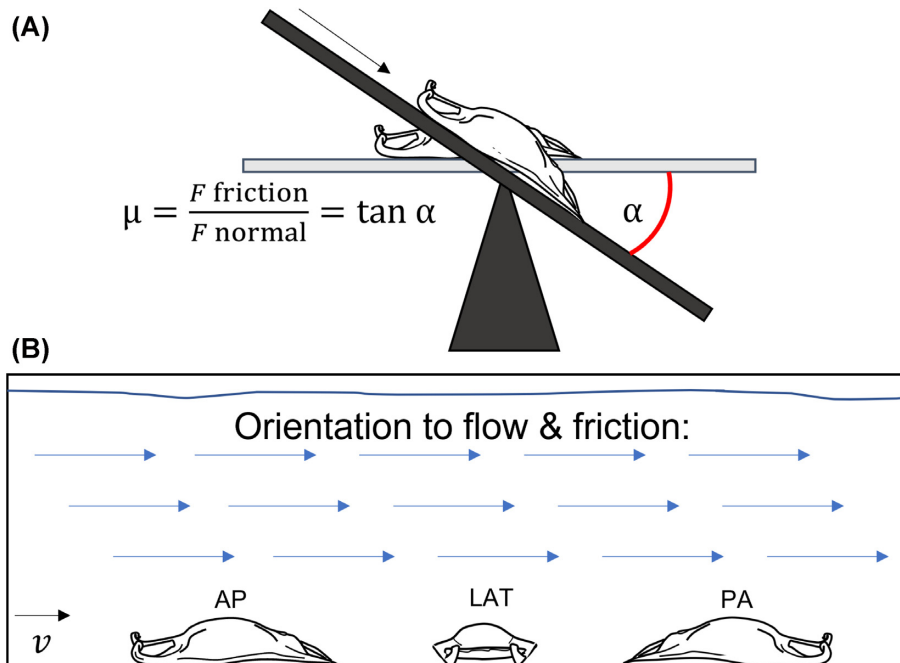


Fig. 3 Methodology to quantify friction and flow. **(A)** We measured the coefficient of friction on the specimens using a motorized metal tilt table. The coefficient of static friction (μ), can be calculated from the angle (α). Egg cases were placed on the tilt table on wet sandpaper to simulate sediment. **(B)** We used a flume to determine the water velocity (cm/s) at which an egg case breaks free of the substrate, blue arrows indicate direction of flow with reference to egg case. The egg cases were tested in three orientations in both the friction and flow trials: Anterior/Posterior (AP), Lateral (LAT), and Posterior/Anterior (PA).

(α ; Ditsche and Summers 2019):

$$\mu = \frac{F_{\text{Friction}}}{F_{\text{Normal}}} = \tan(\alpha).$$

We measured the coefficient of static friction for the eight species, with six different egg cases for five of the species, and three capsules for *B. taranetzi*, *B. minispinosa*, and *R. rhina*. The friction trials were repeated three times for each individual, in all three orientations (anterior/posterior, lateral, and posterior/anterior; Fig. 3B).

Break-away trials

We used a flume with a 152.4 × 38.1 × 50.8 cm working area (Rolling Hills Research Corporation, Model 1520 Water Tunnel) to determine the water velocity at which an egg capsule breaks free of the substrate (break-away velocity, cm/s). Egg cases were placed into a water depth of 35.56 cm, onto the substrate in the orientation of interest without any attachment hardware so that the only thing keeping them in place was the friction between the substrate and the contact surface of the egg case. Each egg case was tested three times, in all three orientations, and the velocity at which the egg broke contact with the substrate was recorded (Fig. 3B). We used the same 60 grit sandpaper substrate in the flume as in the friction measurements, current velocity started at 12.7 cm/s and increased by 2.54 cm/s every 10 s, until the case broke contact with the substrate.

We used R (version 4.1.3, R Core Team 2021), a free coding language for statistics and modeling, via RStudio (RStudio Team 2020), a free integrated development environment (IDE) for R, to estimate drag force for each egg case based on morphometrics. For our drag estimate, we used the equation

$$F_D = \frac{1}{2} A \rho v^2 C_D,$$

where F_D is drag force (N), A is the projected area perpendicular to flow (m²), ρ is the density of seawater (1020 kg/m³), v is free stream flow velocity (cm/s; Vogel 1994), and C_D is drag coefficient (unitless). We estimated C_D using the equation for drag based on thickness ratio:

$$C_D = 1 + 1.5 \left(\frac{h}{w}\right)^{\frac{3}{2}} + 7 \left(\frac{h}{w}\right)^3,$$

where h is the maximum height of the egg case (m) and w is the length of the egg case parallel to flow (m). This equation is derived from measurements of the drag of streamlined shapes based on wetted area from Hoerner (1965): Chapter 6 Drag of Streamline Shapes, equation (28).

Table 1 Linear model results.

Predictor variables	Independent variables		
	AP	PA	LAT
	Species	Species	Species
Friction coefficient	<0.001	0.337	0.154
Estimated drag	<0.001	<0.001	<0.001
Break-away velocity	0.006	<0.001	0.027

Values shown are *P*-values. Abbreviations are as follows: A–P–Anterior/Posterior, P–A–Posterior/Anterior, LAT–Lateral.

Table 2 Linear mixed effect model results.

Predictor variables	Independent variables		
	Friction Coefficient	Break-away Velocity	Estimated Drag
Orientation	0.022	n/a	<0.001
Species	<0.001	0.089	<0.001
Orientation*species	0.011	n/a	0.074
Area	n/a	0.251	n/a
Area*species	n/a	0.007	n/a
Friction coefficient	n/a	n/a	n/a

Values shown are *P*-values.

Scanning electron microscopy

To visualize microstructure, we collected 1 × 1 cm samples from the midline of the ventral surface and the right anterior horn of an egg case from each species (Fig. 4). We stored samples in 70% ETOH, then preserved them in 2% Glutaraldehyde with 0.1M phosphate buffer for 1 h at 22°C. The samples were then rinsed twice in 0.1M phosphate buffered saline for 10 min, we then used an acetone dehydration series before final drying in hexamethyldisilazane (Laforsch and Tollrian 2000; Heiden et al. 2005). We coated samples in gold palladium and imaged them with a NeoScope JCM-5000 scanning electron microscope.

Calculations and statistics

We performed one-way ANOVAs to determine if the coefficient of static friction, break-away velocity, and estimated drag (20 cm/s) (independent variables) were different between species (predictor variable). For these models, data were subset by orientation resulting in nine total models (Table 1). To determine the overall relationship between break-away velocity, coefficient of static friction, and estimated drag (20 cm/s), we created linear mixed effect models using the “lme4” package and ANOVAs using the “car” package in R (Table 2; Bates et al. 2015; Fox and Weisberg 2019). The “lme4” package is designed to fit linear and mixed effect models using Eigen and S4. Please see Bates et al. 2015 for more

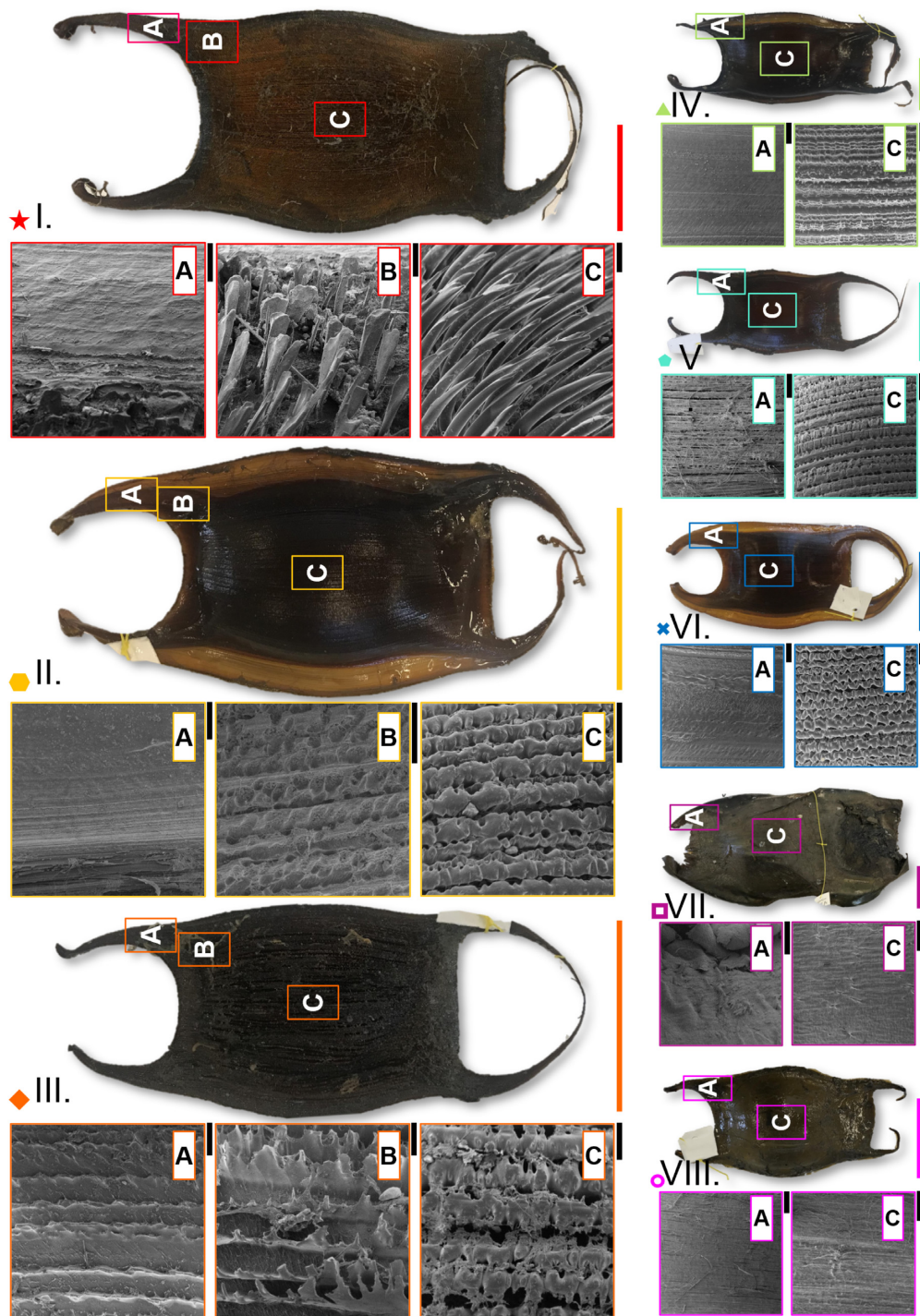


Fig. 4 SEM showing the variation within and among species of egg case microstructure. The samples of 1×1 cm from (A) the right anterior horn, (B) the transitional region between the body capsule to horn, and (C) the midline of the ventral surface. The black SEM scale bar is $500 \mu\text{m}$. The color-coded scale bars for gross morphology are 5 cm. Magenta star—I. *Bathyraja aleutica*, Gold hexagon—II. *Bathyraja interrupta*, Orange diamond—III. *Bathyraja minispinosa*, Lime triangle—IV. *Bathyraja parmifera*, Aqua pentagon—V. *Bathyraja trachura*, Blue X—VI. *Bathyraja taranetzi*, Purple square—VII. *Beringrja binoculata*, and Pink circle—VIII. *Raja rhina*.

information about the implementation of the mixed effect models. For the break-away velocity and the coefficient of static friction models, we used the averages of each independent variable per individual over 2–

3 trials. We created three models. In the first, the coefficient of static friction was the dependent variable, and orientation and species were predictor variables. In the second, break-away velocity was the dependent

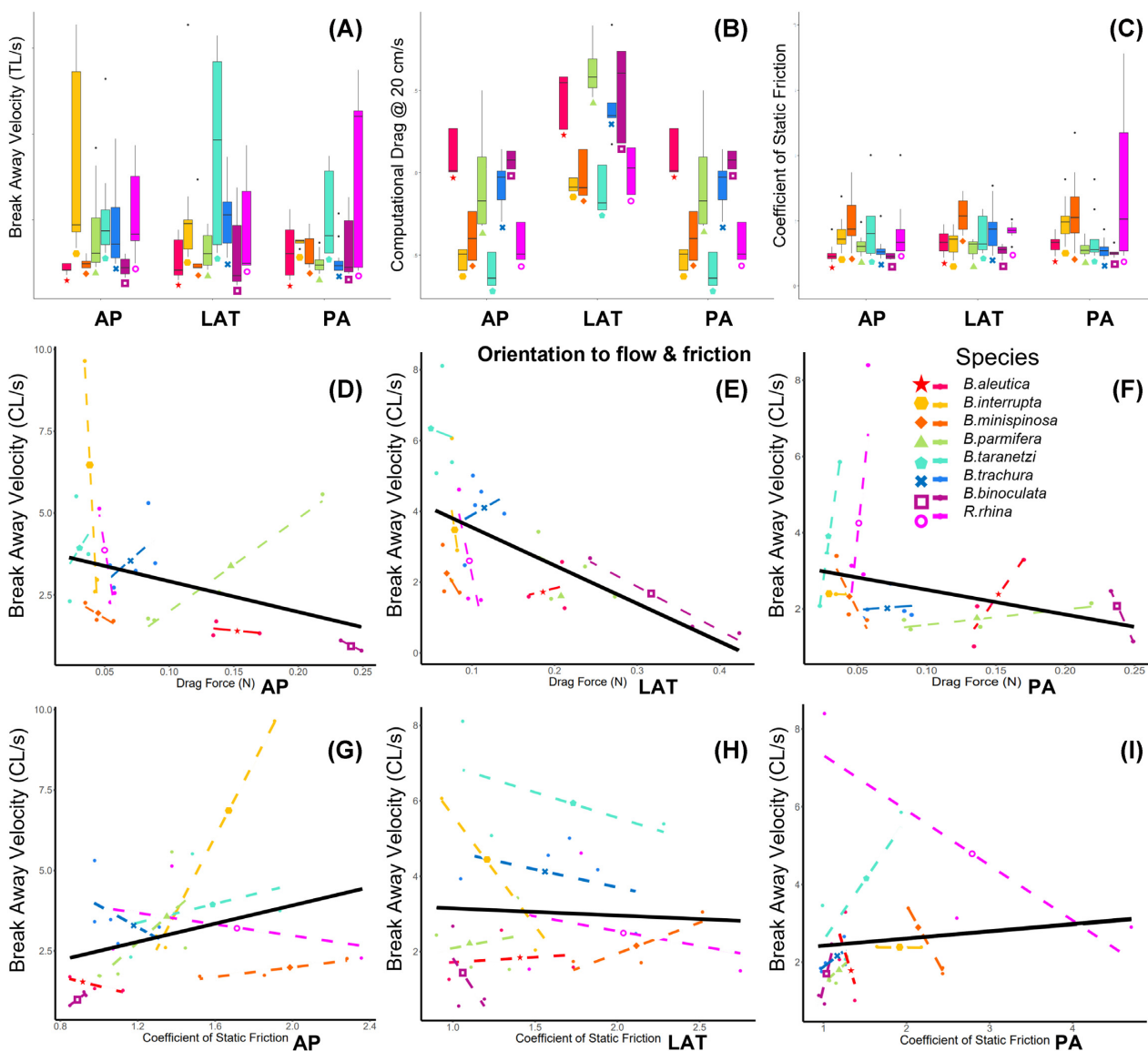


Fig. 5 Friction and flow experimental and computational results. The top panel compares the orientation of egg cases to: **(A)** Break-Away Velocity (cm/s), **(B)** Computational Drag at 20 cm/s, and **(C)** Coefficient of Static Friction. The middle panel compares the relationship between Drag Force (N) and Break-Away Velocity in case length per second (CL/s), in order to standardize for size variation across species in each orientation: **(D)** AP, **(E)** LAT, and **(F)** PA. And the bottom panel compares the relationship between the Coefficient of Static Friction and Break-Away Velocity in case length per second (CL/s), in order to standardize for size variation across species in each orientation: **(G)** AP, **(H)** LAT, and **(I)** PA. The orientation abbreviations are as follows: Anterior/Posterior (AP), Lateral (LAT), and Posterior/Anterior (PA). The black line on **(D–I)** shows the overall trend, which is significant (see [Table 2](#)); the dashed lines represent the specific trend of each species. Genus species are color-coded as follows: Magenta star—I. *Bathyrāja aleutica*, Gold hexagon—II. *Bathyrāja interrupta*, Orange diamond—III. *Bathyrāja minispinosa*, Lime triangle—IV. *Bathyrāja parmifera*, Aqua pentagon—V. *Bathyrāja trachura*, Blue X—VI. *Bathyrāja taranetzi*, Purple square—VII. *Beringrāja binoculata*, and Pink circle—VIII. *Raja rhina*.

variable, and area to flow and species were predictor variables. In the third, estimated drag (20 cm/s) was the dependent variable and orientation and species were predictor variables. In all three models, individual ID was included as a random factor. [Figures 5](#) (experimental data) and [6](#) (environmental data) plots were generated using ggplot2 ([Wickham 2016](#)). A subset of data from Supplementary Table 1 was visualized via

ggplot2 ([Wickham 2016](#)), to show the relationship between depth and current velocity from elasmobranchs found *in situ* in various nursery sites across the globe ([Fig. 6](#)).

Results

We found 20 documented egg case nursery sites across 10 bodies of water in the literature, all of which

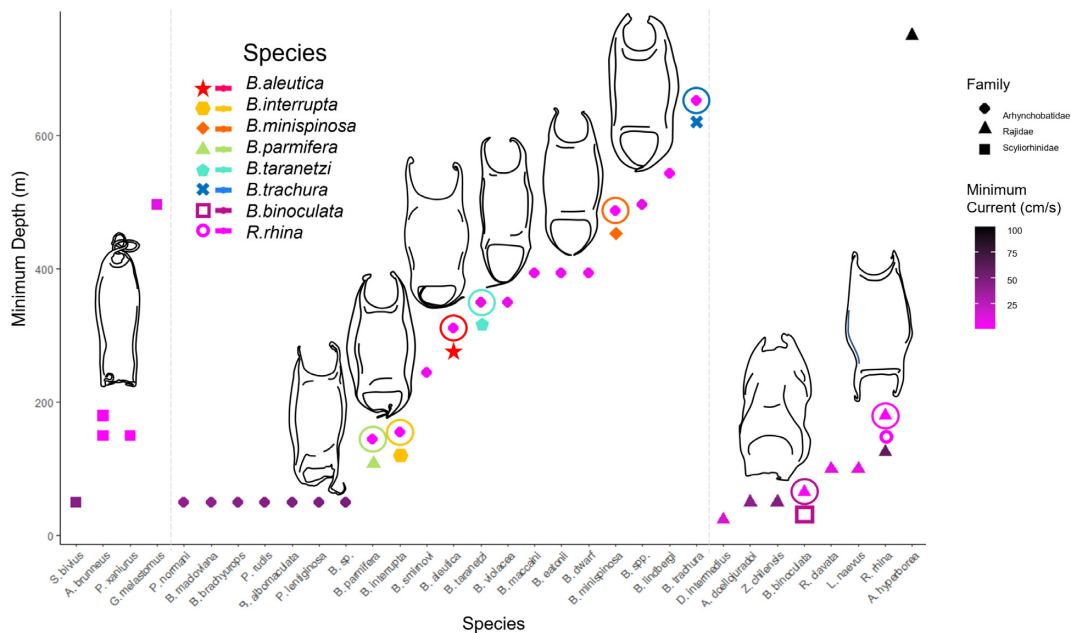


Fig. 6 Range in depth and current velocity that egg cases of each species can withstand. On the graph, from left to right, are the egg cases found at various depths (m), from species of catsharks (Scliorhinidae) shown as squares, softnose skates (Arhynchobatidae) shown as circles, and egg cases from the hardnose skate (Rajidae) shown as triangles. The data points range in color from pink to black, indicating the minimum current (cm/s) they have been found in. Egg case schematics are scaled to each other, not to true size. Circled data points are the color-symbol-coded skate species from this study. These data and literature sources can be found in Supplementary Table 1.

are in regions where coastal upwelling occurs near continental slopes (Fig. 1). Water temperatures at laying sites ranged from 0.25 to 13°C, and depths ranged from 25 to over 1000 m (see Supplementary Table 1). In some places where water was particularly cold, such as the Lofoten–Vesterålen continental margin in Norway, egg cases are laid in cold seeps where the water is warmer than the surroundings (Sen et al. 2019). Sediment type was not consistent across nursery location, rather there is a strong association of nursery sites at the heads of undersea canyons near continental slopes (see Supplementary Table 1).

All nursery sites are deeper than 25 m, with the majority of those being below 50 m (see Supplementary Table 1, Fig. 6). The deepest documented nursery sites are occupied by *B. trachura* (652–1069 m). In most instances, as depth increases, the current velocity decreases. Egg cases are not necessarily limited by current velocity alone; *Amblyraja hyperborea* egg cases are relatively small with non-rigid tapered horns and are found at depths of 750 m, where the current velocity reaches over 100 cm/s.

The egg capsules of many of the eastern Bering Sea and Aleutian species share similar macromorphology, having a short and stout streamlined mid-capsule, and a prominent U-shaped curvature between the anterior horns (Fig. 2). All species have a lateral keel along the edge of the case; this was particularly broad in *B. in-*

errupta and *B. trachura*. The egg cases of *B. aleutica* are longer and wider than the other Alaskan species, but *B. binoculata* is the largest in length, width, and height of all species in this study. The anterior horns are consistently shorter than posterior horns. Aside from case size and shape, the other primary variation between these egg cases is in the posterior horns; some are long and flexible (*B. parmifera*), others are rigid and highly curved inward (*B. aleutica*, *B. minispinosa*, *B. trachura*). The two posterior horn oddities of this dataset are *B. binoculata*, which lacks a posterior gap because the apron continues to the bottom of each horn, and *R. rhina*, in which the horns hook ventrally, versus medially as in other species (Fig. 2).

There is variation in the surface microstructure both within a single capsule and among species (Fig. 4). For example, *B. aleutica* has thorn-like projections which transition to paddle-like structures near the anterior horn, and the horn itself is smooth with a few ridges (Figs. 4I. A, B, and C). Also, *B. minispinosa* has lobular notches that make up the longitudinal ridges on the main body of the capsule, but the transitional zone (body to horn) exhibits thin and jagged longitudinal ridges, and the horns have short sharp ridges (Figs. 4III. A, B, and C). There is also variation between species, for example the two species that co-occur in the Salish Sea, *B. binoculata* and *R. rhina*, both lack longitudinal ridges, and while *B. binoculata* cases are smooth, *R. rhina* cases

have thin, string-like fibers (Figs. 4VII. A and C; 4VIII. A and C).

There is also variation in the performance measures—coefficient of static friction and break-away velocity—within a single capsule and among capsules from different species. But these relationships are not simple. For example, break-away velocity is predicted by the interaction of area and species, but not area or species alone. The coefficient of static friction is predicted by species, but not orientation. Our finding that break-away velocity is predicted by the interaction of area, species, and the coefficient of static friction (Tables 1 and 2, Figs. 5G, H, and I) indicates that microstructure does influence the ability to stay stuck, since friction is largely determined by microstructure. But friction alone does not account for how those species stay stuck on a similar substrate, as the coefficient of static friction was not significant for the posterior and lateral orientations (Table 1). Further, the computational estimated drag (20 cm/s) also determines whether the shape of a species will be significantly different from other species in variable nursery sites and experimental habitats (Table 1).

Discussion

Here we investigated the hydrodynamic properties of egg cases deposited by skates of the eastern North Pacific. Our results suggest that orientation and surface microstructure influence the ability of an egg case to adhere to the substrate, thus maintaining its position in favorable current velocity and conditions that favor circulation of oxygen flow through the egg case during their long developmental period.

The constant temperature and high nutrient load of submarine canyons, driven by coastal upwelling, provides an excellent environment for the long, slow development process of skates (Luchin et al. 1999; Hoff 2008). Skate egg cases need several things for successful development. These include exposure to a narrow range of temperatures over a multiple-year time frame, well-oxygenated water, and, for post-hatching nutrition, an abundance of small invertebrate prey. Upwelling sites provide all these resources. Egg cases can take 1–4 years to develop and for much of this time the embryo gets oxygen from water that flows through the capsule, driven by surrounding currents (Koob and Summers 1996; Long and Koob 1997; Hoff 2008). The complex topography at the heads of canyons ensures a current flow with well-oxygenated water from the mixing of the ocean thermocline (Sigler et al. 2015; Ropper et al. 2019). Eggs must be found in regions with moderate currents to create sufficient water flow across the egg surface to sustain metabolic processes

(Leonard et al. 1999; Hoff 2007, 2008) and ensure eggs are not covered with sediments. When the embryo finally hatches it has a small amount of yolk, but it must start eating soon. Prey, usually small invertebrates like copepods and amphipods, are common on the nutrient-rich seafloor around an upwelling area (Springer et al. 1996; Stabeno et al. 1999; Whitley and Luchin 1999). Similarly, mothers are more likely to deposit eggs in habitats where food is guaranteed, so that they can eat and replenish their own energy stores before the next reproductive cycle (Hoff 2008).

Although we regularly find egg cases for *B. binoculata* and *R. rhina* in the Puget Sound and Salish Sea, the abiotic factors relevant for a highly populated nursery site do not exist consistently enough in this location. Based on seafloor topography, slower current velocity, and depth range we propose that a nursery site for *R. rhina* is likely to occur off the coast of Victoria, Canada in the Juan de Fuca Canyon (Fig. 1, blue dot). Two alternative locations for nursery sites would be the Quinault Canyon and Astoria Canyon off the coast of northern Washington. The findings of Hitz (1964) and our study support the notion that *B. binoculata* should lay their eggs in regions with slower currents because their cases perform worse in high current systems than *R. rhina*. It is interesting to note a contradiction in morphology and performance (Figs. 5 and 6) for *B. binoculata*. The asymmetrical capsule, with dorsal keels (see Supplementary Fig. 1), suggests that this species would perform better in higher currents; instead, we found that *B. binoculata* has one of the lowest abilities to withstand high flow in both experimental and mathematical testing. These results support the one *in situ* encounter of a *B. binoculata* nursery site, where eggs were found relatively shallow at 65 m, in currents under 13 cm/s (see Supplementary Table 1, Fig. 6). The current velocity within and around the San Juan Archipelago are notoriously fast at 1–3 m/s (Yang et al. 2021), illustrating why we find solitary egg cases, not dozens to hundreds of cases in one location.

One thing to note is the apparent dichotomy between species that live in a shallower environment vs a deeper one (Fig. 6; Hoff 2009). Shallower species (*B. parmifera*, *B. interrupta*, *B. taranetzi*) all have a relatively similar morphology with distinct lateral keels, smooth surfaces, and shallow nursery sites (Figs. 2, 4, and 6). The other *Bathyrāja* species (*B. aleutica*, *B. minispinosa*) found in deeper nursery sites tend to have narrow lateral keels and a complex surface microstructure. The one exception to this trend, between deep and shallow species, is *B. trachura* which is a deep-water species with egg cases that are morphologically similar to the shallow species. This dichotomy could be the basis for further

investigation into the relationship between case morphology and habitat preference.

We found that friction is not the only thing that determines case mobility or lack thereof (Figs. 5G, H, and I). Once deposited from the mother, the cases, are covered in a sticky thread-like material which functions to pick up particulates (shells, substrate, etc.) from the surrounding environment (Koob 1999). This allows the egg case to settle securely into the substrate and resist fast and fluctuating currents (Koob 1999; Compagno 2001; Rocha et al. 2010). The collection of particles may contribute to the case's ability to stay in place. The sticky attachment fibrils of *B. binocularata* are a mat-like pad atop the posterior apron (see Supplementary Fig. 1), we found that this fibrous-mat seemed to function as a weighted anchor to keep the case in contact with the substrate, as this case morphology lacks "true horns" that might otherwise attach to structures. In addition to the gross morphology and microstructures, these horns and fibrous tendrils, are additional systems used to anchor or attach the case to the substrate and allow the eggs to remain in unlikely high-current habitats (Love et al. 2008; Graiff et al. 2016). Unlike skates, mother catsharks (Scyliorhinidae) are known to intentionally wrap the tendrils of the candle-shaped egg cases around kelp stalks to keep them in place (Pretorius 2012; Hiscock et al. 2019). For species that lack tendrils, such as *A. hyperborea*, females may prioritize other secure substrates, such as tubeworm fields and other sessile invertebrates, that the cases can grip onto (see Supplementary Table 1; Sen et al. 2019). The egg cases of *A. hyperborea* are relatively small with non-rigid tapered horns and are found at depths of 750 m, where current velocity reaches over 100 cm/s (Fig. 6; Åström et al. 2020; Sen et al. 2019). These species are capable of remaining attached in such a high current system because the mothers prioritize sites with copious amounts of tubeworms and other structure-forming marine invertebrates to keep them anchored to the nursery area (see Supplementary Table 1; Graiff et al. 2016).

Further research incorporating the life-history of the taxa in question, their biology, and biomechanics would aid in fine-tuning the predictive models for future habitat protection plans. Cross-referencing, species ranges, canyons, and upwelling zones will optimize where to survey via submersible camera systems (ROV, Fernandez-Arcaya et al. 2017; Bernhardt and Schwanghart 2021). Pinpointing habitat hotspots, or essential fish habitats will supply the data needed to validate policy regulations as to where longline limitations should be imposed. These regions should be made the top priority in protective fisheries management proposals in the future.

Acknowledgments

We thank D. Stevenson and J. Hoff of the National Oceanic and Atmospheric Administration's Alaska Fisheries Science Center for the Alaskan species egg cases collected during the eastern Bering Sea bottom trawl survey. We thank Dr. Stacy Farina for leading the 2019 cohort of researchers. Lastly, we thank the Washington Department of Fish and Wildlife for Salish Sea species egg cases and the Friday Harbor Laboratories (FHL) Kittiwake.

Funding

This work was supported by the NSF-REU and FHL Blinks-Beacon for funding JNE. And the Stephen and Ruth Wainwright Endowed Fellowship, BEACON and Hoag Awards, Robert T. Paine Experimental and Field Ecology Award, FHL Award, FHL Marine Science Fund, FHL Student Fund (Kohn), Patricia L. Dudley Endowment for funding KCH.

Supplementary data

Supplementary data available at *ICB* online.

Conflicts of interest

None.

Data availability statement

All data will be housed/available for public viewing and downloading in this googlefolder: <https://docs.google.com/spreadsheets/d/1TZHoU08erodYvWcSsmDpnFnnvGVMwnX4/edit?usp=sharing&ouid=112694120904919400715&rtopof=true&sd=true>.

References

- Åström EK, Sen A, Carroll ML, Carroll J. 2020. Cold Seeps in a warming Arctic: insights for benthic ecology. *Front Mar Sci* 7:244.
- Atwood TB, Witt A, Mayorga J, Hammill E, Sala E. 2020. Global patterns in marine sediment carbon stocks. *Front Mar Sci* 7:165.
- Bates D, Mächler M, Bolker B, Walker S. 2015. Fitting linear mixed-effects models using lme4. *J Stat Softw* 67:1–48.
- Bernhardt A, Schwanghart W. 2021. Where and why do submarine canyons remain connected to the shore during sea-level rise? Insights from global topographic analysis and Bayesian regression. *Geophys Res Lett* 48:e2020GL092234.
- Bowden FP, Tabor D. 1950. *The friction and lubrication of solids*. Oxford: Clarendon Press.
- Chiquillo KL, Ebert DA, Slager CJ, Crow KD. 2014. The secret of the mermaid's purse: phylogenetic affinities within the Rajidae and the evolution of a novel reproductive strategy in skates. *Mol Phylogenet Evol* 75:245–51.

- Compagno LJ. 2001. Sharks of the world: bullhead, mackerel, and carpet sharks (Heterodontiformes, Lamniformes, and Orectolobiformes). Vol. 4. New Delhi: Food and Agriculture Organization.
- Core Team R. 2021. R: a language and environment for statistical computing. Vienna: R Foundation for Statistical Computing.
- Ditsche P, Summers A. 2019. Learning from northern clingfish (*Gobiesox maeandricus*): bioinspired suction cups attach to rough surfaces. *Philos Trans R Soc B: Biol Sci* 374: 20190204.
- Ebert DA, Winton MV. 2010. Chondrichthyans of high latitude seas. In: Carrier Jeffery C, Musick John A, Heithaus Michael R., editors. The biology of sharks and their relatives. Vol. 2. Boca Raton (FL): CRC Press.
- Fernandez-Arcaya U, Ramirez-Llodra E, Aguzzi J, Allcock AL, Davies JS, Dissanayake A, Harris P, Howell K, Huvenne VA, Macmillan-Lawler M, et al. 2017. Ecological role of submarine canyons and need for canyon conservation: a review. *Front Mar Sci* 4:5.
- Fox J, Weisberg S. 2019. An R companion to applied regression. 3rd ed. Thousand Oaks (CA): Sage.
- Graiff K, Lipski DM, Etnoyer PJ, Cochrane GR, Williams GC, Salgado E. 2016. Benthic characterization of deep-water habitat in the newly expanded areas of Cordell Bank and Greater Farallones National Marine Sanctuaries. NOAA Institutional Repository ONMS-16-01.
- Heiden TCK, Haines AN, Manire C, Lombardi J, Koob TJ. 2005. Structure and permeability of the egg capsule of the bonnethead shark, *Sphyrna tiburo*. *J Exp Zool A Comp Exp Biol* 303A:577–89.
- Hiscock K, Christie H, Bekkby T. 2019. The ecology of the rocky subtidal habitats of the northeast Atlantic. In: Hawkins SJ, Bohn K, Firth LB, Williams GA, editors. Interactions in the marine benthos: global patterns and processes. Cambridge: Cambridge University Press.
- Hitz CR. 1964. Observations on egg cases of the big skate (*Raja binoculata* Girard) found in Oregon coastal waters. *J Fish Res Board Can* 21:851–4.
- Hoerner SF. 1965. Fluid-dynamic drag. Hoerner fluid dynamics. Published by the author.
- Hoff GR. 2007. Reproductive biology of the Alaska skate *Bathyraja parmifera*, with regard to nursery sites, embryo development and predation [dissertation]. [Seattle (WA)]: University of Washington.
- Hoff GR. 2008. A nursery site of the Alaska skate (*Bathyraja parmifera*) in the eastern Bering Sea. *Fish Bull* 106:233–44.
- Hoff GR. 2009. Skate *Bathyraja* spp. egg predation in the eastern Bering Sea. *J Fish Biol* 74:250–69.
- Hoff GR. 2010. Identification of skate nursery habitat in the eastern Bering Sea. *Mar Ecol Prog Ser* 403:243–54.
- Hoff GR. 2016. Identification of multiple nursery habitats of skates in the eastern Bering Sea. *J Fish Biol* 88:1746–57.
- Ishihara H, Treloar M, Bor PH, Senou H, Jeong C. 2012. The comparative morphology of skate egg capsules (Chondrichthyes: Elasmobranchii: Rajiformes). *Bull Kanagawa Prefect Mus (Nat Sci)* 41:9–25.
- Koob TJ, Summers A. 1996. On the hydrodynamic shape of little skate (*Raja erinacea*) egg capsules. *Bull Mt Desert Isl Biol Lab* 35:108–11.
- Koob TJ. 1999. Female reproductive system. Sharks, skates, and rays: the biology of elasmobranch fishes. JHU Press. p.398.
- Laforsch C, Tollrian R. 2000. A new preparation technique of daphnids for scanning electron microscopy using hexamethyldisilazane. *Archiv für Hydrobiologie* 149:587–96.
- Leonard JB, Summers AP, Koob TJ. 1999. Metabolic rate of embryonic little skate, *Raja erinacea* (Chondrichthyes: Batoidea): the cost of active pumping. *J Exp Zool* 283:13–8.
- Long JH, Koob TJ. 1997. Ventilating the skate egg capsule: the transitory tail pump of embryonic little skates (*Raja erinacea*). *Bull Mt Desert Is Biol Lab* 36:117–9.
- Love MS, Schroeder DM, Snook L, York A, Cochrane G. 2008. All their eggs in one basket: a rocky reef nursery for the longnose skate (*Raja rhina* Jordan & Gilbert, 1880) in the southern California Bight. Vol. 106. Fishery Bulletin, 471–5.
- Luchin VA, Menovshchikov VA, Lavrentiev VM, Reed RK. 1999. Thermohaline structure and water masses in the Bering Sea. In: Loughlin TR, Ohtani K, editors. Dynamics of the Bering Sea, AK-SG-99-03, Fairbanks, AK: University of Alaska Sea Grant College Program. p. 61–91.
- Melton S, Kelly SR, Witherell D, Eagleton M, Olson JV, Ellgen S, Hansen K, Hoff GR, Ormseth OA, Kenne AJ, et al. 2014. Final Environmental Assessment for Amendment 104 to the Fishery Management Plan for Groundfish of the Bering Sea and Aleutian Islands Management Area Habitat Areas of Particular Concern (HAPC) Areas of Skate Egg Concentration December 2014.
- Pretorius CA. 2012. Factors influencing the development and mortality rate of shy and cat shark embryos in South African waters [dissertation]. [Cape Town]: University of Cape Town.
- Reichert AN. 2020. Habitat associations of catshark egg cases (Chondrichthyes: Carcharhiniformes: Pentanchidae) from the US Pacific Coast. Master's Theses at Digital Commons @ CSUMB: California State University Monterey Bay.
- Rocha F, Oddone MC, Gadig OB. 2010. Egg capsules of the little skate, *Psammodontus obsoletus* (Garman, 1913) (Chondrichthyes, Rajidae). *Braz J Oceanogr* 58:251–4.
- Rooper CN, Hoff GR, Stevenson DE, Orr JW, Spies IB. 2019. Skate egg nursery habitat in the eastern Bering Sea: a predictive model. *Mar Ecol Prog Ser* 609:163–78.
- RStudio Team. 2020. RStudio: integrated development for R. Boston (MA): RStudio, PBC.
- Schindelin J, Arganda-Carreras I, Frise E, Kaynig V, Longair M, Pietzsch T, Preibisch S, Rueden C, Saalfeld S, Schmid B, et al. 2012. Fiji: an open-source platform for biological-image analysis. *Nat Methods* 9:676–82.
- Sen A, Himmler T, Hong WL, Chitkara C, Lee RW, Ferré B, Lepland A, Knies J. 2019. Atypical biological features of a new cold seep site on the Lofoten-Vesterålen continental margin (northern Norway). *Sci Rep* 9:1–14.
- Sigler MF, Rooper CN, Hoff GR, Stone RP, McConnaughey RA, Wilderbuer TK. 2015. Faunal features of submarine canyons on the eastern Bering Sea slope. *Mar Ecol Prog Ser* 526:21–40.
- Springer AM, McROY CP, Flint MV. 1996. The Bering Sea Green Belt: shelf-edge processes and ecosystem production. *Fish Oceanogr* 5:205–23.
- Stabeno PJ, Schumacher JD, Ohtani K. 1999. The physical oceanography of the Bering Sea. *Dynamics of the Bering Sea* 1–28.
- Stevenson DE, Hoff GR, Orr JW, Spies IB, Rooper CN. 2019. Interactions between fisheries and early life stages of skates in nursery areas of the eastern Bering Sea. *Fish Bull* 117: 8–14.

- Stevenson DE, Orr JW, Hoff GR, McEachran JD. 2007. Field guide to sharks, skates, and ratfish of Alaska. Anchorage (AK): Alaska Sea Grant College Program.
- Vogel S. 1994. Life in moving fluids: the physical biology of flow. Princeton (NJ): Princeton University Press.
- Whitledge TE, Luchin VA. 1999. Summary of chemical distribution and dynamics in the Bering Sea. In *Dynamics of the Bering Sea* 217–49.
- Wickham H. 2016. *Ggplot2: elegant graphics for data analysis*. New York (NY): Springer-Verlag.
- Wourms JP. 1977. Reproduction and development in chondrichthyan fishes. *Am Zool* 17: 379–410.
- Yang Z, Wang T, Branch R, Xiao Z, Deb M. 2021. Tidal stream energy resource characterization in the Salish Sea. *Renew Energy* 172:188–208.